

Scene-Based Atmospheric Correction Methods for LWIR Hyperspectral Sensors.

F. Leaver, O. Thomas
Thales Optronics, Thorpe Road
Staines, TW18 3HP

Abstract

Three methods for atmospheric correction have been evaluated with data captured with the AHI sensor. Techniques for the separation of the effects of temperature and emissivity have also been examined to account for the contribution of reflected downwelling radiance to the measured signature.

Keywords: ISAC, AAC, Blackwell, ARTEMISS, Gillespie

Introduction

The infrared emitted radiation from the ground surface and targets is absorbed or scattered by the atmosphere before it reaches an airborne or land based hyperspectral sensor. The atmosphere distorts spectral signatures and measured LWIR hyperspectral signatures of a particular object/material vary enormously since they are dependent on object/material temperature, the environmental conditions and range and look angle. Corruption of the signature means that the observed signal cannot be matched to signatures of known targets in a spectral library i.e. targets cannot be identified.

Target detection with LWIR hyperspectral data requires real-time scene-based atmospheric correction.

Current methods have not been fully evaluated for military applications. These methods include In-Scene Atmospheric Correction (ISAC), Autonomous Atmospheric Compensation (AAC) and the method of Blackwell. Temperature Emissivity Separation (TES) accounts for downwelling radiance.

Atmospheric correction

The radiance measured by a LWIR hyperspectral sensor (L_m) may be expressed as the transfer equation:

$$L_m = \varepsilon B(\lambda, T)\tau + (1 - \varepsilon)L_d\tau + L_u$$

where ε is the pixel emissivity, τ is the atmospheric transmittance, L_d is the atmospheric downwelling radiance, L_u is the atmospheric path radiance and $B(\lambda, T)$ is the Planck expression in wavelength and temperature for blackbody radiation. The goal is to determine the emissivity given only the measured radiation. Correction for path radiance and transmittance ignores the middle term on the right hand side.

ISAC algorithm

The In-Scene Atmospheric Correction algorithm [1] works by, for each wavelength, fitting a line to the top of the scatterplot of measured pixel radiation versus blackbody radiation given an assumed pixel temperature. At the top of the scatterplot lie the actual blackbodies and the gradient of the line is the atmospheric transmittance while the vertical intercept is

the path radiance. An example of the output of automatic line fitting to the top of the scatterplot is seen in Figure 1.

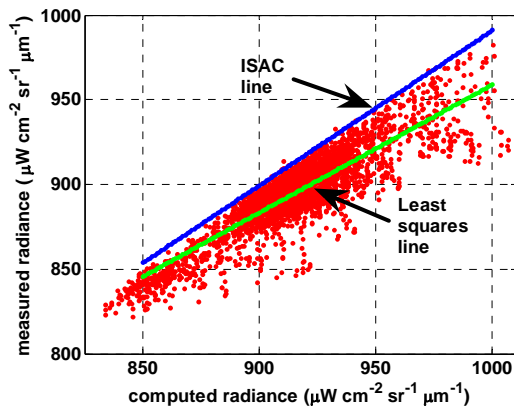


Figure 1 ISAC line fit

AAC algorithm

The autonomous atmospheric compensation algorithm [2] characterises the entire atmosphere radiometrically in LWIR in terms of parameters describing the strong water absorption channel at 11.7 microns.

Transmittance ratio and path difference parameters are defined as

$$Tr = \frac{\tau(\lambda_s)}{\tau(\lambda_w)}$$

$$Pd = L_{path}(\lambda_s) - TrL_{path}(\lambda_w)$$

where λ_s and λ_w are respectively the wavelengths within the absorption channel and on the outside edge of the absorption channel.

Expressions for transmittance and path radiance of the form

$$y(\lambda) = \sum_{i=1}^3 \sum_{j=1}^3 C_{ij}(\lambda) Tr^{i-1} Pd^{j-1}$$

are trained using data generated with the MODTRAN atmospheric modelling code.

The AHI data employed do not contain the 11.7-micron absorption channel. Experiments with a weaker absorption channel were undertaken but correction results were poor. This may be due to the increased relative effects of noise.

Algorithm of Blackwell

The algorithm of Blackwell [3] maps observed radiation to vertical profiles for atmospheric temperature and relative humidity using a neural network and then passes the profiles into MODTRAN to generate transmittance, path radiance and downwelling radiance. These are used within the transfer equation to yield emissivity.

ARTEMIS TES

The atmospheric correction offered by ISAC and AAC necessarily ignores reflected downwelling radiance. The result of subtraction of path radiance and division by transmittance is the sum of emitted and reflected radiances. Isolation of the emissivity requires estimation of the downwelling radiance. Within the ARTEMIS (Automatic Retrieval of Temperature and Emissivity using Spectral Smoothness) algorithm [4] a set of atmospheres is identified based upon correlation of the derived ISAC or AAC transmittance with the transmittance component of the individual atmospheres in a library. Downwelling radiance is selected by identifying the individual atmosphere that delivers the smoothest emissivities given individual optimisation of each pixel temperature.

TES of Gillespie et al

The inputs to the TES of Gillespie et al [5] are the downwelling radiance and the sums

of emitted and reflected pixel radiation (i.e. correction for path radiance and transmittance has been undertaken) for an individual pixel. Temperature and emissivity are adjusted iteratively until the recovered radiance changes no more. Rescaling of the emissivity and deployment of an empirical equation serve to deliver a final emissivity result. The algorithm is illustrated in Figure 2.

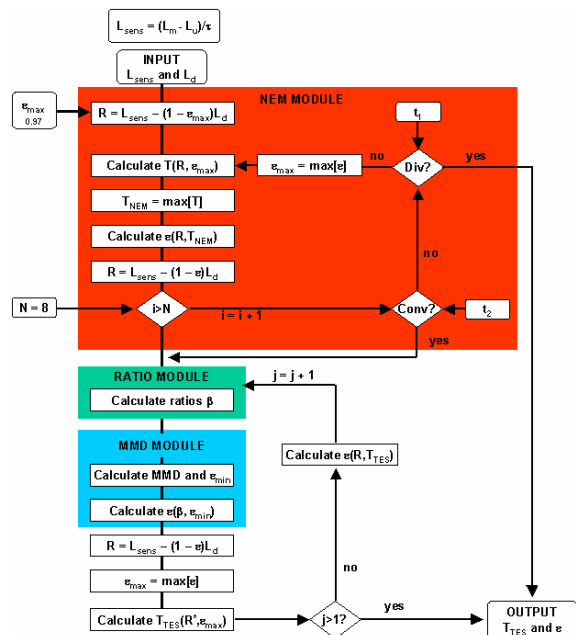


Figure 2 Flow diagram for TES of Gillespie et al

Integrated architecture

The AHI data do not encompass the strong 11.7-micron water absorption channel that is key to the AAC algorithm. This channel can also be used within the ISAC algorithm to rescale the spectra for transmittance and path radiance. This limitation has motivated the linking together of the numerous processes to allow the generation of meaningful output. The algorithms may potentially be linked together to provide emissivity (ϵ) and temperature (T) as illustrated in Figure 3.

The ISAC algorithm provides unscaled atmospheric transmittance. This can be

correlated with the corresponding components in the library of atmospheres within the ARTEMIS process. The downwelling radiance of the best match of atmosphere within ARTEMIS can be passed as an input to the method of Gillespie. The correction of the observed radiance with the ISAC outputs is also passed to the method of Gillespie as an input.

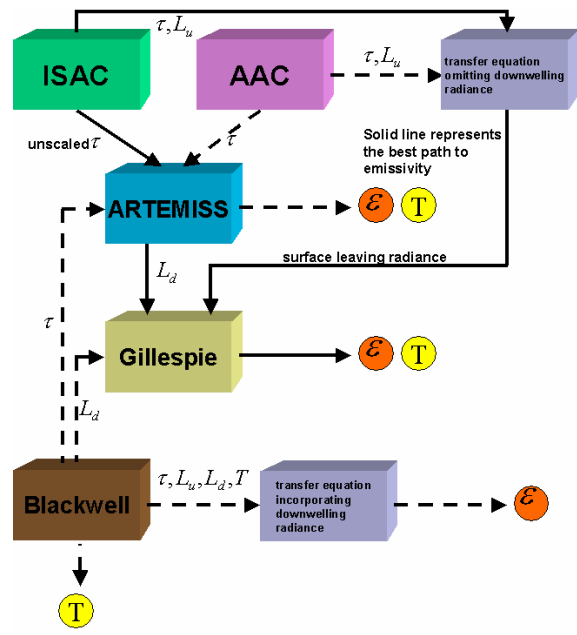


Figure 3 Integrated architecture

The absence of scaling of the ISAC outputs does not prevent use of these to correct the data from which they were derived. The Blackwell algorithm can deliver temperature and emissivity by itself or could provide inputs to the TES processes.

Scene analysed

Known emissivities in the AHI data were few. Consequently attention was focused on part of the trials-site containing pools of water. This is illustrated in Figure 4.

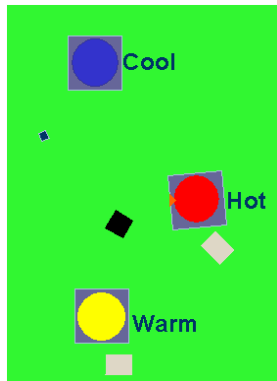


Figure 4 Scene analysed

The emissivity of water is found readily in the literature. The pools of water were placed in a flat gravel area and the emissivity of this type of material was also available to the project. The pools are placed on square sheets laid upon the gravel area. The “cool” pool is unheated.

Emissivity recovery

Water pixel emissivities recovered using the method of Gillespie are seen in Figure 6. Note the vertical scale starts at 0.8.

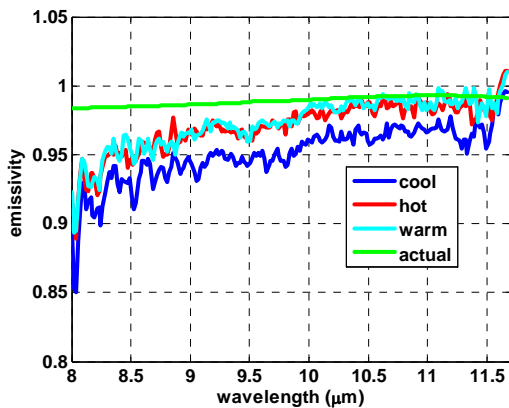


Figure 6 Water pixel emissivities

The emissivity of a gravel pixel in the same scene has been determined by the methods of Gillespie and ARTEMIS and is seen in the Figure 7.

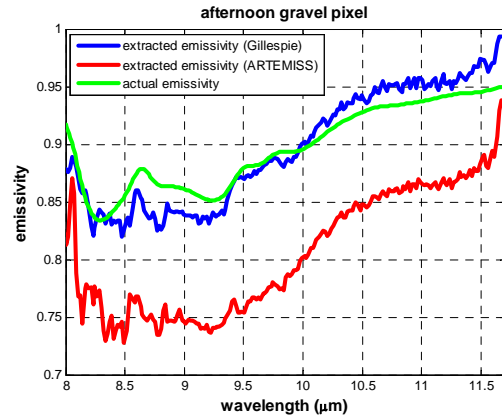


Figure 7 Gravel pixel emissivity

The ARTEMIS emissivity is poor while the Gillespie result compares well.

Scene emissivity analysis

K-means clustering has been employed in an unsupervised classification of the radiance and Gillespie emissivity cubes. The results are displayed in Figure 8.

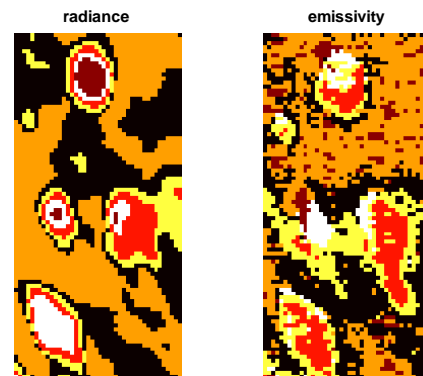


Figure 8 Result of K-means analysis

The pools in the radiance cube are deemed to be of different compositions while in the emissivity cube the pools have similar compositions. Known emissivities for water and gravel have been used in a spectral angle mapper analysis of the scene. An RGB interpretation of the result is seen in Figure 9.

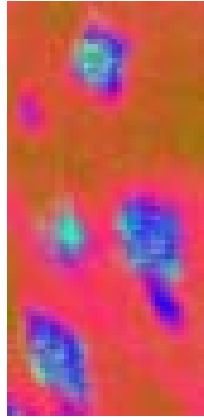


Figure 9 SAM analysis

The blue channel represents the water-like, the red the gravel-like and the green channel is assigned to a measure of neither water nor gravel.

Results from method of Blackwell

Neural networks have been trained to provide vertical profiles for atmospheric temperature and relative humidity given an observed radiance. The relative humidity delivered by the method of Blackwell is seen here in Figure 10 with the actual profile.

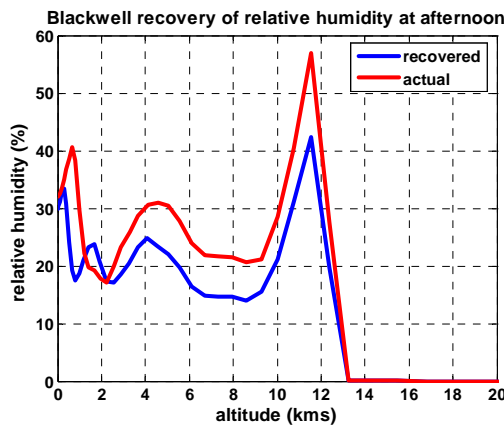


Figure 10 Humidity profile

The atmospheric temperature profile delivered by the method Blackwell is seen in Figure 11 together with the actual profile.

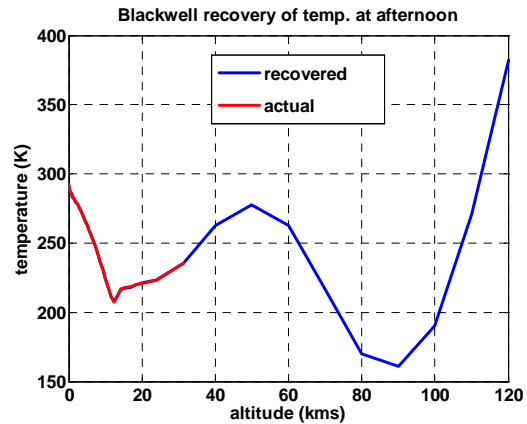


Figure 11 Temperature profile

The humidity profile match is poor which is possibly due to insufficient variation in the training data. The temperature profile appears to be a good match. The use of these profiles within MODTRAN has delivered the atmospheric spectra for use with the inversion of the transfer equation to yield emissivity. The emissivity for a gravel pixel so determined is shown in Figure 12. Equivalent results to the Blackwell approach can be achieved using randomly selected atmospheres from the training library and these results are shown also.

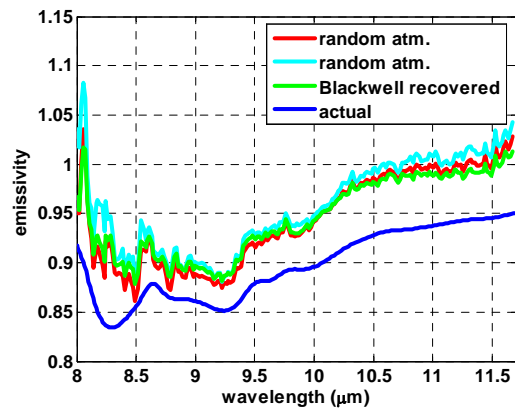


Figure 12 Blackwell gravel emissivities

Scene temperature recovery

The TES processes and the method of Blackwell are able to provide calculation of the temperatures of the scene pixels. An example of the temperatures in the pool

scene determined by these algorithms is shown in Figure 13.

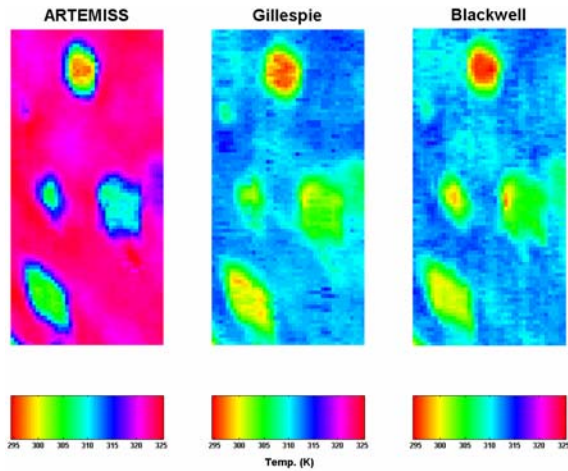


Figure 13 Pixel temperature maps

ARTEMISS overestimates the temperature of the background. The methods of Gillespie and Blackwell provide similar temperature outputs and in respect of the pools of water deliver results that lie between the estimates provided by the two ground truth sensors.

Conclusions

This paper has described the implementation and testing of three quite different processes for characterisation of the atmosphere and the subsequent use of these outputs in two different processes for the delivery of pixel emissivity. Many of the recovered emissivities exhibit some residual atmospheric/noise effects that potentially may introduce uncertainty into the spectral matching process. Nonetheless, spectral matching has been seen to be effective in scene analysis with these data. The nature of the hyperspectral data analysed has limited the application of the conclusions that may be drawn with respect to LWIR data in general. The AHI data set is missing information in the important 11.7-micron water absorption channel employed in the AAC algorithm and in the scaling process within the ISAC approach. The performance of AAC has undoubtedly

suffered through the use of a weaker absorption notch and the ISAC results have not been rescaleable. The algorithm architecture ultimately developed has allowed correction of the data despite these shortcomings and both AAC and ISAC have provided inputs for the temperature emissivity separation processes. A qualitative rating of the processes is offered (stars out of five).

Correction & TES	Rating
ISAC - ARTEMISS	**
ISAC – ART. - Gillespie	*****
AAC - ARTEMISS	*
AAC – ART. - Gillespie	***
Blackwell – trfr. equation	*****

References

- 1 Young, S., Johnson, R. and Hackwell, J., Journal of Geophysical Research, Vol. 107, No. D24, 2002
- 2 Gu et al, IEEE Transactions on Geoscience and Remote Sensing, Vol. 38, No. 6, 2000
- 3 Blackwell, W., Proceedings of SPIE Vol. 5425, 2004
- 4 Borel, C.C., 28th Annual GOMACTech Conference, Hyperspectral Imaging Session, 2003, Florida
- 5 Gillespie et al, IEEE Transactions on Geoscience and Remote Sensing, Vol. 36, No. 4, 1998

Acknowledgements

The work reported in this paper was funded by the Electro-Magnetic Remote Sensing (EMRS) Defence Technology Centre, established by the UK Ministry of Defence and run by a consortium of Selex Sensors and Airborne Systems, Thales Defence, Roke Manor Research and Filtronic.

Thales Optronics is grateful to DSTL for supplying the data employed on this project.